# Interlaced x-ray microplanar beams: A radiosurgery approach with clinical potential

F. Avraham Dilmanian[a,b], Zhong Zhong[c], Tigran Bacarian[a,d], Helene Benveniste[a,e], Pantaleo Romanelli[a,f,g], Ruiliang Wang[h], Jeremy Welwart[a], Tetsuya Yuasa[a,i], Eliot M. Rosen[j], and David J. Anschel[a,f]

[a]Medical and [h]Chemistry Departments and [c]National Synchrotron Light Source, Brookhaven National Laboratory, Upton, NY 11973; Departments of [e]Anesthesiology and [f]Neurology, State University of New York, Stony Brook, NY 11794; [g]Department of Neurosurgery, Istituto di Ricovero e Cura a Carattere Scientifico (IRCCS) Neuromed Medical Center, IS 86077 Pozzilli, Italy; and [j]Lombardi Comprehensive Cancer Center, Georgetown University, Washington, DC 20057

Communicated by Richard B. Setlow, Brookhaven National Laboratory, Upton, NY, May 2, 2006 (received for review January 24, 2006)

**Studies have shown that x-rays delivered as arrays of parallel microplanar beams (microbeams), 25- to 90-$\mu$m thick and spaced 100–300 $\mu$m on-center, respectively, spare normal tissues including the central nervous system (CNS) and preferentially damage tumors. However, such thin microbeams can only be produced by synchrotron sources and have other practical limitations to clinical implementation. To approach this problem, we first studied CNS tolerance to much thicker beams. Three of four rats whose spinal cords were exposed transaxially to four 400-Gy, 0.68-mm microbeams, spaced 4 mm, and all four rats irradiated to their brains with large, 170-Gy arrays of such beams spaced 1.36 mm, all observed for 7 months, showed no paralysis or behavioral changes. We then used an interlacing geometry in which two such arrays at a 90° angle produced the equivalent of a contiguous beam in the target volume only. By using this approach, we produced 90-, 120-, and 150-Gy 3.4 × 3.4 × 3.4 mm$^3$ exposures in the rat brain. MRIs performed 6 months later revealed focal damage within the target volume at the 120- and 150-Gy doses but no apparent damage elsewhere at 120 Gy. Monte Carlo calculations indicated a 30-$\mu$m dose falloff (80–20%) at the edge of the target, which is much less than the 2- to 5-mm value for conventional radiotherapy and radiosurgery. These findings strongly suggest potential application of interlaced microbeams to treat tumors or to ablate nontumorous abnormalities with minimal damage to surrounding normal tissue.**

radiation therapy | synchrotron x rays | tissue repair | tissue sparing | x-ray microbeam

The fundamental limitation of conventional radiotherapy is the risk of long-term damage to healthy tissue. Microbeam radiation therapy (MRT) is an experimental approach that has produced, in single exposures, exceptionally high tolerance in the normal tissues while preferentially damaging malignant tumors. MRT employs parallel arrays of microscopically thin planar beams of synchrotron-generated x-rays [microplanar beams or microbeams (MBs)] (1–16). MRT research is being pursued both at the National Synchrotron Light Source at the Brookhaven National Laboratory, where the method was initiated (1), and at the European Synchrotron Radiation Facility (Grenoble, France). Most MRT studies have used very thin, 25–90 $\mu$m, MBs spaced 100–300 $\mu$m on-center, respectively.

Prior studies have shown that irradiation of rats with 9LGS malignant brain tumors[k] (2, 7, 15) and mice with s.c. EMT-6 murine mammary carcinomas (8) and SCCVII murine squamous cell carcinoma (14) with unidirectional, single-fraction, high dose, thin-beam MRT preferentially damages the tumors while sparing healthy tissue. This unexpected and unique preferential tumoricidal effect has become the hallmark of the MRT approach. Thus, MRT yielded a higher therapeutic index (ratio of maximum dose tolerated by normal tissue to minimum dose required to control the tumor) than nonsegmented beams of a similar energy spectrum (7, 8).

The biological mechanisms through which MRT spares normal tissue and preferentially kills tumors are still poorly understood. One hypothesis that has received experimental support is the rapid regeneration of normal microvessels damaged in the direct paths of thin MBs (1, 6, 10, 16). The MBs' preferential tumoricidal effects, or strong tumor palliation properties, are due, in part, to the lack of recovery of the tumor vasculature[l] (2, 7, 8), presumably because of structural differences between microvessels of tumor and those of the surrounding normal tissue (17).

The tolerance of normal tissues to unidirectional MB arrays has been confirmed in the following animal models at the indicated maximum in-beam incident dose: (*i*) adult rat brain (800 Gy; refs. 1, 2, 7, and 11), (*ii*) suckling rat cerebellum (150 Gy; ref. 3), (*iii*) piglet cerebellum (600 Gy; ref. 4), (*iv*) duckling embryo brain (160 Gy; ref. 5), and (*v*) skin and muscle of the mouse leg (970 Gy; refs. 8 and 14) and rat leg (1,000 Gy; ref. 9). All these studies demonstrate "robustness" of the method's normal-tissue sparing. Recently, we also demonstrated that a single 270-$\mu$m-thick MB at a 750-Gy-depth dose is well tolerated in the normal rat brain and spinal cord (11). In fact, the irradiation induced remyelination and repopulation of glial cells within 3 months, an effect that may find future therapeutic application in itself (11).

The previous MRT studies, using median beam energies of up to 120 keV only (1 eV = $1.602 \times 10^{-19}$ J), demonstrated that the response of the normal tissue and tumor critically depends on the dose distribution produced by the MB arrays in the exposed tissue. Compton scattering and photoelectric events that set electrons in motion produce the dose, and Monte Carlo simulations are used to calculate the MRT dose distributions (18–21).

Although "thin-beam" MBs (and their associated small beam-spacing) are candidates for clinical use in major synchrotron laboratories, they have limitations to their widespread clinical implementation. First, they can be produced only by synchrotron sources. Second, they require low-energy beams (<200-keV median energy), thus limiting dose penetration to the tissue. The reason is that if the range in the tissue of the photoelectrons and Compton electrons set in motion by incident photons is much larger

Conflict of interest statement: No conflicts declared.

Abbreviations: MB, microbeam; MRT, MB radiation therapy.

[b]To whom correspondence should be addressed. E-mail: dilmanian@bnl.gov.

[d]Present address: University of California, Irvine, CA 92697

[i]Permanent address: Faculty of Engineering, University of Yamagata, Yamagata, Japan.

[k]Morris, G., Zhong, N., Bacarian, T., Coderre, J., Peña, L., Recksiek, P., Rosen, E., Robinson, J., Tammam, T. & Dilmanian, A. (2001) *National Synchrotron Light Source Activity Report 2000*, eds. Corwin, M. A. & Ehrlich, S. N. (Brookhaven Natl. Lab., Upton, NY), abstr. Morr6526.

[l]Dilmanian, F. A., Hainfeld, J. F., Kruse, C. A., Cool, C. D., Sze, C.-I., Laterra, J. S., Feldman, A., Gatley, S. J., Nawrocky, M. M. & Yakupov, R. (2003) *National Synchrotron Light Source Activity Report 2002*, eds. Corwin, M. A. & Ehrlich, S. N. (Brookhaven Natl. Lab., Upton, NY), abstr. Dilm0599.

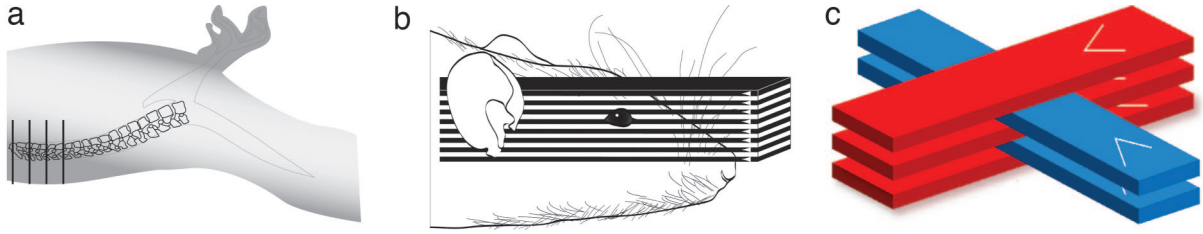


**Fig. 1.** Schematic demonstration of irradiations with MB arrays. (*a*) Rat spinal cord irradiations with four MBs. (*b*) Rat brain irradiation with a large array of MBs. (*c*) Interlaced MBs.

than the thickness of the MBs, the nearly rectangular-shaped dose distribution produced by each MB will develop broad shoulders (11) that fill in the dose in the "valley" regions of the dose distribution (i.e., the regions between the direct MBs to which radiation leaks). For example, 200-keV photons will produce shoulders of ≈30 $\mu$m on the sides of 30-$\mu$m-thick beams (11). Third, narrow MBs are vulnerable to beam smearing from cardiosynchronous tissue pulsation (22). Finally, the clinical implementation of the interlaced method producing a broad beam at the target introduced here is virtually impossible with very thin beams because of demanding mechanical tolerances. The thick-MB approach presented here ameliorates these limitations.

Recently, Bräuer-Krisch *et al.* (12, 13) at the European Synchrotron Radiation Facility proposed an approach in which two arrays of 25-$\mu$m-thick beams spaced at 211 $\mu$m apart were interlaced at the target to generate an array of MBs with half-beam spacing. The method increased the valley dose in the target 3-fold compared with that from a single array. This approach is different from that presented here because it uses thin MBs, and it does not produce a contiguous beam in the target.

The description of the highly nonuniform dose of MRT, particularly that in the interlaced-MBs configuration, requires terminology beyond that used in conventional-beam dosimetry. Although all doses relate to energy per unit mass, the sampling volumes involved are very small. Besides the more common terms, such as incident dose and depth dose, this work uses "peak dose" (which is the same as "in-beam dose"), "valley dose," and "integrated dose" (dose integrated over one or several cycles of the MB arrays).

## Results

**Tolerance of the Spinal Cord to Thick MBs.** Rats were transaxially irradiated in their thoracic spinal cord with four parallel MBs, 0.27, 0.37, 0.5, and 0.68 mm thick, spaced 4 mm on-center at an in-beam depth dose of 400 Gy (Fig. 1*a*). They were observed for 7 months for signs of paralysis, weighed, and assessed by using the rotarod test (23, 24). This time point was chosen because it is assumed to cover the manifestation of much of the delayed radiation effects in the rat's CNS (25). Only one rat in the 0.68-mm group was killed, 13 days after irradiation, because of signs of paralysis; the three remaining rats exhibited leg weakness between days 10 and 20 after irradiation; however, they all regained their leg strength by 1 month after irradiation. Fig. 2 *a* and *b* compare the average weight and rotarod performance of the three surviving rats with those of the unirradiated control animals. The irradiated rats lagged behind unirradiated controls in weight by ≈50 g, a difference that continued for the entire 7 months (Fig. 2*a*). However, their rotarod performance reached control levels by ≈1 month after irradiation (compare Fig. 2*b*). After 5 months the rotarod performance declined in both the irradiated and control rats, probably due to their weight gains and/or aging. Although the rats in the 0.5-mm group did not show any apparent weakness in the legs or significant loss in their rotarod performance, one rat in that group died for unknown reasons 202 days after irradiation with no sign of paralysis. The rats in the 0.27- and 0.37-mm groups showed no and little weight loss, respectively (see Fig. 2*a* for the latter) and no temporary decline in their rotarod performance.

In another study, rats were similarly irradiated by using a 7-mm-wide contiguous unsegmented beam,[k] except that the irradiation site was the cervical spinal cord rather than the thoracic cord. The in-beam depth doses tested were 25, 50, and 75 Gy, using groups of four to six rats each. Three of six rats that received 75 Gy became paralyzed and were killed within 3 months, producing an $ED_{50}$ (dose for 50% effect) of 122 days. A fourth rat lost weight and became partially paralyzed around the same time but recovered 2 months later. All three surviving rats in the 75-Gy group were observed for 1 year and did very poorly in the rotarod test. One of four rats in the 50-Gy group died at 10 months after irradiation. The rats in both the 25- and 50-Gy groups performed less well on the rotarod test than the unirradiated control rats. These studies show the advantage of MBs over broad beams in their tolerance by the spinal cord.

**Tolerance of the Rat Brain to Thick MB Arrays.** Rats were irradiated over nearly their entire brain unilaterally (in the anteroposterior

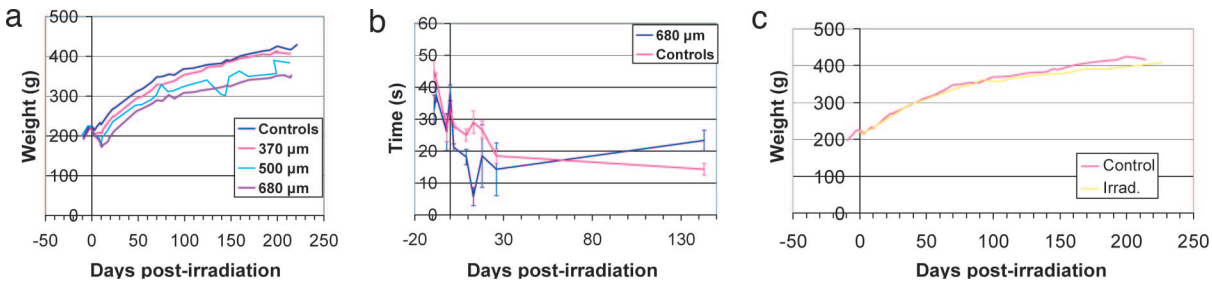


**Fig. 2.** Results of the studies with the rat spinal cord and brain. (*a*) Averaged weights as a function of time of rats irradiated in their spinal cord with sets of four parallel MBs at 400 Gy and 0.68-, 0.50-, and 0.37-mm thickness compared with the controls. (*b*) Average rotarod performance of the rats in the 0.68-mm group above compared with the controls. (*c*) Average weights of the rats irradiated in their brain with a 170-Gy array of 0.68-mm beams spaced 1.36 mm on-center compared with the controls.

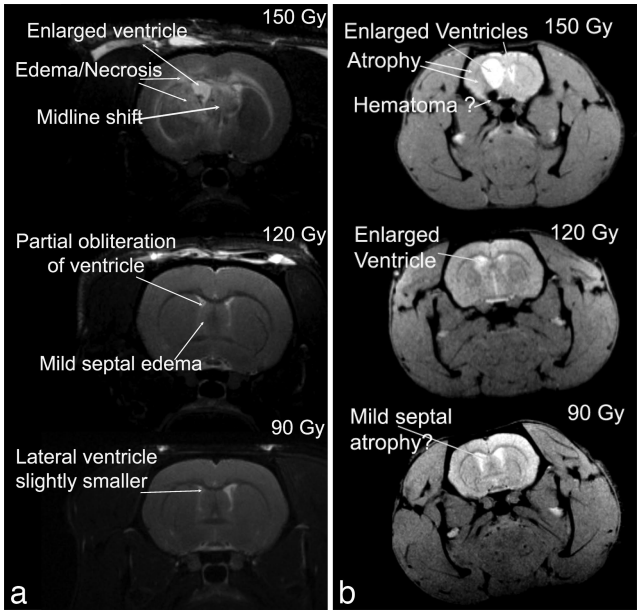


**Fig. 3.** MRI images of the rats irradiated in their brain with an interlaced array of MBs at 90-, 120-, and 150-Gy depth doses 3 weeks (*a*) (T2-weighted) and 6 months (*b*) (T2*-weighted) after the irradiation.

direction) using an array of 0.68-mm-thick MBs spaced 1.36 mm on-center. The array was 8 mm wide × 10.2 mm tall (schematics in Fig. 1*b*). In-beam incident doses of 110, 130, 150, and 170 Gy were used. Two of the four rats in the 170-Gy group exhibited a behavioral episode of moving around in an abnormal way, which started ≈3 h after irradiation and ended ≈2 h later. The rats, observed for 7 months, gained weight normally (Fig. 2*c*) and did not show signs of limb weakness at any time.

**Dose Localization by Interlaced Thick MBs.** Rats were irradiated with interlaced MBs in a cubic region of 3.4 × 3.4 × 3.4 $mm^3$ close to their right motor cortex using two arrays of 0.68-mm beams spaced 1.36 mm at 90-, 120-, and 150-Gy-depth doses (schematic in Fig. 1*c*). All rats behaved normally. T2-weighted MRI images were acquired at 3 weeks, and T2*-weighted images were acquired at 6 months after irradiation for one rat in each group (Fig. 3). The MRI results are summarized in Table 1. Acutely, 150 Gy produces extensive damage to the target site, with some edema tracking along the corpus callosum in the contralateral side. The edema outside the target resolves over time (compare Fig. 3 *a* and *b*). The 120-Gy dose seems to produce a "nearly perfect" microlesion. The apparent damage is limited to the target site. Outside the target area it produced minimal edema, which resolved by 6 months (Fig. 3). The effects of 90 Gy are very subtle within the target region, with no apparent changes on the contralateral side at either of the two time points.

**Dose Distribution Calculations for Clinical Scenarios.** Monte Carlo simulations using the code EGS4 (26–28) were used to assess dose distributions for arrays of interlacing MBs, 0.68 mm thick, spaced 1.36 mm apart, in phantoms relevant to clinical situations. In one simulation, 1.5 × 1.5-cm arrays were aimed at the center of a 12 × 12-cm spherical water phantom resembling a small tumor in the neck. The resulting valley-to-peak dose ratio was 13.5% in one array 1 cm from the edge of the target.

The second simulation, which was designed to resemble a small brain tumor, used two arrays of 3 × 3 cm each aimed at the center of a 16 × 16-cm cylindrical water phantom (see schematic view in Fig. 4*a*). The dose profiles at the center of the cubic interlaced region and in the noninterlaced region 1 cm from the interlacing edge are shown in Fig. 4 *b* and *c*, respectively. Here the valley-to-peak dose ratio is ≈17% (Fig. 4*b*); it decreases with increasing distance from the target. For this phantom and for a beam with 4.5-cm tissue half-value layer, a 50-Gy dose at the center of the interlaced volume will produce ≈15-Gy valley dose 1 cm proximal to the side of the 3-cm-side cubic target (at a peak dose of 73 Gy). This valley dose can be reduced by using two dose fractions. Another significant finding of this study was that the dose at the edge of the target fell very sharply, with an 80–20% dose falloff of only 30 μm (Fig. 4*b*). The corresponding dose falloff in conventional radiation therapy is 2–5 mm.

## Discussion

We found that irradiation of the rat spinal cord with four parallel 0.68-mm-thick MBs at 400 Gy in-beam depth dose was tolerated, long-term, in three of four rats, as evaluated by weight gains and rotarod performance. In contrast, a similar study in which the cervical spinal cord was exposed to 7-mm-long broad-beam[k] showed much smaller tolerance. Likewise, other investigators found an $ED_{50}$ of 19 Gy for paralysis in Fischer 344 rats 7 months after a single-fraction, 20-mm-wide exposure of their spinal cord to x-rays (29, 30). Although the experimental designs of these studies were not identical, a cursory comparison suggests that the spinal cord has greater tolerance to the thick MBs compared with the unsegmented beams. Quantitatively, the "integrated dose" (see definition above) of the MBs in this study (assuming

**Table 1. Summary of MRI results**

| | Early effects* | | Late effects† | |
|---|---|---|---|---|
| Dose, Gy | Target region | Contralateral hemisphere | Target region | Contralateral hemisphere |
| 150 | Edema with midline shift; parenchymal damage; enlarged ventricles | Edema tracking along the corpus callosum; septal damage; slightly enlarged ventricles | Atrophy of the neocortex, striatum and septum; enlarged ventricles/hydrocephalus; small low-signal intensity area suggestive of hematoma | Septal atrophy; enlarged ventricles |
| 120 | Mild septal edema; partial obliteration of lateral ventricle | No apparent changes | "Nearly perfect" microlesion | No apparent changes |
| 90 | Lateral ventricular space slightly reduced | No apparent changes | No apparent changes | No apparent changes |

See Fig. 3 for more details.
*Three weeks (Fig. 3*a*).
†Six months (Fig. 3*b*).

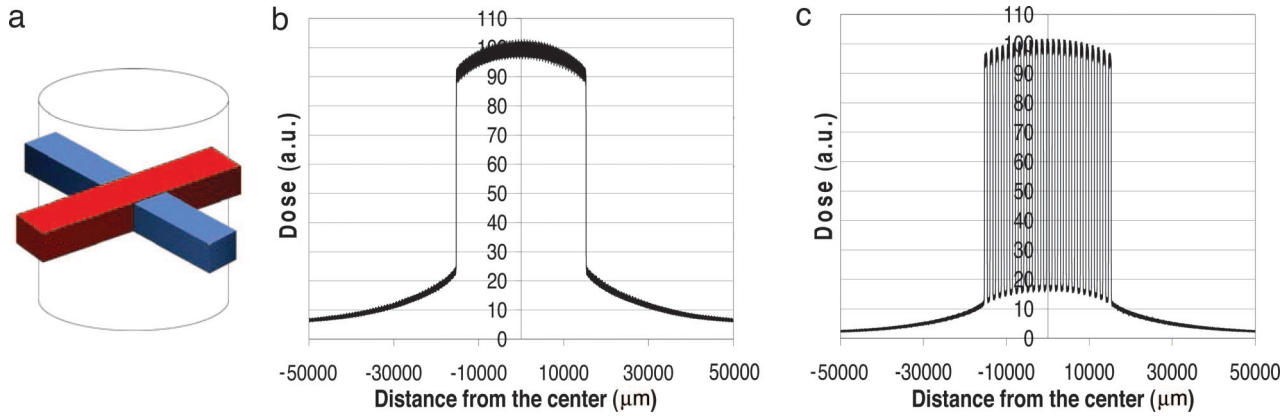


**Fig. 4.** EGS4 Monte Carlo simulation of two 3 × 3-cm arrays of MBs interlacing at the center of a 16 × 16-cm cylindrical water phantom. (*a*) Schematic view. (*b* and *c*) Dose profiles are shown at the center of the interlaced region (*b*) and in the noninterlaced region 1 cm from the interlacing edge (*c*). a.u., arbitrary units.

a 2% valley dose) is 76 Gy, which is close to the 75-Gy dose in our unsegmented-beam study that paralyzed four of six rats in 3 months, and is much larger than our 25- and 50-Gy unsegmented beams that caused sensorimotor dysfunction in a year.

Although some spinal cord damage resulted from the 0.68- and 0.5-mm beams at 400 Gy, these beams would clearly be tolerable at the lower doses that would be relevant to clinical radiation therapy. In this regard, the 0.68-mm beam might be the threshold where the tissue's tolerance rapidly decreases with increasing beam thickness. In support of this statement, H. Curtis (31), who was the first investigator to report the MB effect with ionizing radiation, demonstrated a complete destruction of the mouse cerebellum tissue with 1-mm-diameter, 25-MeV deuteron beams at 140 Gy in 240 days. A possible explanation for the sudden reduction in the tolerable dose with thicker beams might be that the "biological component" of the effect [which is known to have the essential element of vascular repair (1, 6, 10)] disappears, and only the "volume effect" (32) stays.

In our rat brain study, we found that a large, unilateral array of parallel 0.68-mm-thick MBs spaced 1.36 mm on-center is well tolerated by the rat brain at in-beam incident doses of up to 170 Gy. The hyperactivity observed shortly after irradiation of the rats in the 170-Gy group may be due to a temporary increase of the intracranial pressure, given the large irradiation field and dose, in addition to the relatively small ratio of beam spacing to beam thickness (2:1) compared with the 3:1 to 8:1 range used in previous MRT studies that raises the valley dose. However, the long-term results suggest that the valley dose was not excessive. We estimate that the MBs' in-depth integrated dose, assuming an 11% valley dose and a 4.5-cm tissue half-value layer, was 88 Gy. Other investigators exposing the rat brain to a single dose of contiguous unsegmented x-ray beams using a semicircular lead aperture of 10 mm radius found $ED_{50}$ values for necrosis in white matter of 23 Gy at 39 weeks and 21 Gy at 52 weeks (33, 34). Dividing the 88-Gy integrated dose by the average of these two doses (i.e., 22 Gy), we find a radiation tolerance advantage of 4.0-fold or higher for our beams (because our dose is not for $ED_{50}$). This tolerance advantage factor is similar to a reported one of 4.2-fold for thin MBs in the rat brain (7).

Finally, the MRI results from our interlaced MB study of the rat brain revealed significant edema and parenchymal damage to the target area only in the 150-Gy group acutely and ensuing atrophy at 6 months. Importantly, the contralateral hemisphere of the 150-Gy-exposed rat demonstrated mild edema acutely, which was resolved at 6 months. This observation is remarkable considering the excessive dose used. Neither the 120- nor 90-Gy groups exhibited significant damage outside the target area at any time, indicating that these doses are well tolerated. Clearly, the MRI findings of this study are potentially clinically relevant because MRI is used as a gold standard to assess brain damage after radiation treatments in humans.

Our findings have implications for potential clinical use of MBs. Thicker MBs may allow the use of higher-energy photons from a possible special x-ray tube without the need for synchrotron source. The higher beam energy, in turn, will increase the depth of dose penetration (thus lowering the dose to the proximal tissue) and will have a more significant "skin-sparing effect" compared with that from the lower beam energies used with thin MBs. The thicker beams also will relax the mechanical tolerances needed to implement the interlacing of the two arrays. Finally, because the interlaced method presented here produces an unsegmented beam at target, the doses required to control tumors will be much lower that those required with noninterlaced MBs.

The interlaced MB method of Brauer-Krisch *et al.* (12, 13), compared with that presented here, has the benefits of exploiting the preferential tumoricidal effect of MRT, whereas our approach has other advantages (i.e., thicker MBs, an unsegmented beam at the target, lower dose) but does not make use of MBs' preferential tumor killing.

As indicated in the introduction, the normal-tissue tolerance to MBs critically depends on the MBs' dose distributions. First, for any given dose, the beam thickness should not exceed a certain width. Second, for a given beam thickness, the valley dose should be minimized; it increases with an increasing ratio of MB thickness to beam spacing, array size, subject size, and tissue depth. Finally, the peak dose should be lower than the dose that kills neurons in the direct path of the MBs (1–4, 11). Our Monte Carlo simulations suggest that the valley dose from interlacing thick MB arrays may be sufficiently low to spare the nontargeted tissue in single-fraction treatment of human brain tumors of up to ≈27 $cm^3$. However, a lower valley dose might be possible by delivering the dose in two fractions spaced 1–3 days apart, by using perpendicular (or nearly perpendicular) symmetry axes in the two dose-delivery patterns. In this geometry, only one array from the second irradiation will intersect an earlier array, and that will be at a right angle; a beam intersecting that should be tolerable given the superior and fast ability of normal tissue to recover from MBs.

The sharper beam edge from synchrotron radiation results, in part, from the quasiparallel nature of the beam and the small effective synchrotron source spot size. By comparison, dose falloffs of 2–5 mm are produced by x-rays derived from megavoltage medical linear accelerators (35–37) or from gamma ray sources

(37–39); they are caused by the long range in tissue of the high-energy Compton electrons and by the 1.5- to 2-mm typical source spot size as well as the small distances between the radiation source and collimator used under treatment conditions.

For generation of thick MBs similar to those used in the present study, a bremsstrahlung source conceivably might provide the required beam energy, intensity, and source size. In this respect, beams with median energy of up to 250–300 keV (with x-ray tubes operating at up to ≈450 kVp) might become feasible. This would be "intermediate-beam energy" for radiation therapy, compared with "low energy" synchrotron-generated thin MBs and "high-energy" linac x-ray or Co-60 gamma rays from Gamma Knife.

The 30-$\mu$m 80–20% dose falloff our simulations predict for synchrotron x-rays of 120-keV-median energy would be increased to ≈0.2–0.5 mm with orthovoltage beam. It depends on the kVp setting, the beam filtration, the source spot size, and the distances between the source, the MB collimator, and the subject.

Theoretical advantages of using interlaced thick MBs over the existing clinical radiotherapy and radiosurgery methods include the following: (*i*) improved normal tissue tolerance because of exposure of normal tissue to noninterlaced MBs; (*ii*) a smaller dose falloff distance at the edge of the beam, which will reduce the dose to the normal tissue and is particularly advantageous for small targets near sensitive organs; and (*iii*) potentially more effective combination with tumor-dose-enhancement agents based on intermediate and high *Z*-contrast elements, because of the larger photoelectric cross section of the MRT's lower beam energies. The latter techniques include photon activation therapy (40, 41) and the use of dose-enhancing contrast agents, such as iodine (42, 43), platinum (41), and gold (44, 45). A disadvantage of the interlaced method would be the limited number of beam entrance portals around the tumor, which reduce the ability to conform the dose to the target. This ability would be important for targets of irregular shapes.

If proven effective clinically, the interlacing MB approach could open up several possibilities. First, because of its lower impact on the nontargeted tissue, it might allow the use of higher, potentially curative doses in those clinical cases in which cure is not possible today. Second, it might allow retreatment of the CNS months or years after the initial treatment(s), as well as the treatment of pediatric CNS tumors. Third, the sharp dose falloff of the method could provide for "microradiosurgery," with more highly localized deposition of the dose, especially for small- and medium-sized targets. Such applications might include stereotactic treatment of (*i*) noncancerous disorders such as arteriovenous malformations, epilepsy, and movement disorders especially (i.e., Parkinson's disease, tremor) and (*ii*) tumors positioned near very sensitive organs such as ocular melanoma, pituitary adenoma, and tumors of the spinal cord. Finally, our approach might allow for the temporary disruption of the bloodbrain barrier in very small brain regions (10–20 $mm^3$) for selective delivery of a drug to the brain (46).

## Materials and Methods

The rats were treated humanely in accordance with the guidelines set by the U.S. Department of Agriculture and Brookhaven National Laboratory. All rats were purchased from Taconic Farms and were 12 weeks old at the time of irradiation. They were anesthetized with xylazine (9 mg/kg) and ketamine (55 mg/kg) for irradiation.

**Irradiation Setup.** The irradiations were carried out at the National Synchrotron Light Source X17B1 superconducting wiggler beamline. The National Synchrotron Light Source X-Ray Electron Storage Ring operates at 2.8-GeV energy, and the beamline's wiggler is at 4.3 T. Filtration of the beam with 1/4-inch Cu produced a dose rate of 40 Gy/s (in average) at a median energy of 120 keV. The source spot size is elliptical, 0.9 mm wide horizontally and 0.05 mm high vertically. The subject is positioned 30 m from the source and 15 cm from the collimator.

**Rat Spinal Cord Irradiation with Thick MBs.** Fischer 344 rats were positioned supine, with their backs horizontally positioned on a wooden stage and their spines aligned perpendicular to the horizontally propagating synchrotron beam. They were irradiated transaxially to the spine with arrays of four parallel vertical MBs of the same thickness, spaced 4 mm center-to-center, centered on the T9 vertebra. The incident dose in all irradiation was 530 Gy, which corresponds to 400 Gy in-beam depth dose (estimating the beam's attenuation in tissue proximal to the spinal cord to be ≈25%). Four groups of four rats each were irradiated using beam thickness values of 0.27, 0.37, 0.5, and 0.68 mm. These values were chosen to include the 0.27-mm (13) and 0.5-mm (arbitrary choice) values and to be equally spaced logarithmically (a 1.36:1.0 ratio between each two values). The MBs were 18 mm tall, starting from the wooden bed, and were produced by nine 2-mm-tall vertical tiers. The complete irradiation time for each rat was ≈8 min. This irradiation geometry assured that the beams crossed the spinal cord as they did in an earlier study in which histological examinations confirmed the spinal cord exposure (11). Seven unirradiated rats were used as controls. In a study of unsegmented beams from the same synchrotron source that was carried out earlier,[k] male Fischer 344 rats were irradiated to the cervical spinal cord with 7-mm-wide beams.

**Rat Brain Irradiation with Unidirectional Thick MBs.** Fischer 344 rats were positioned in the beam prone, facing the beam, with the back of their head placed horizontally and the rest of their body bent downward to avoid exposure to the spinal cord. They were irradiated anteroposteriorly (i.e., rostral-to-caudal), with an 8-mm wide × 10.2-mm tall array of parallel horizontal MBs of 0.68-mm beam thickness and 1.36-mm beam spacing (i.e., 8 beams). Four groups of four rats each were irradiated by using single-exposure doses of 110-, 130-, 150-, and 170-Gy in-beam incident doses. The arrays were centered 3 mm to the left of the midline and started from the top of the brain. The irradiation time was ≈40 s for rats in the 170-Gy group.

**Rat Brain Irradiated with Interlaced MBs.** Sprague–Dawley rats were positioned vertically in the beam using a plastic head-frame. To align the brain with the beam, using the bregma as the landmark and a laser beam that showed the center of the x-ray beam, the skull was exposed surgically. The head-frame then was fixed to a table capable of submillimeter computer-guided movement in two orthogonal planes. After aligning the bregma with the laser beam, we moved the rat to the left by 2.5 mm, and the back-to-front exposure was made with three parallel horizontal MBs, with 3.4-mm array width. The frame was then rotated 90°, so that the right side of the head faced the beam, and was adjusted in its new lateral position so that the left side of the array was on the interface between the skull and the top of the brain (i.e., at the edge of the cortex). The stage then was moved vertically upward by 0.65 mm (i.e., half of the 1.30 mm chosen beam spacing, on-center) to make the lateral exposure, composed of two parallel MBs, with the same 3.4-mm array width, interlace with the first one. In-beam depth doses of 90, 120, and 150 Gy were used with two rats in each group. The exposure time was <1 min for all doses.

**Follow-Up.** The rotarod method (23, 24) employs a rugged horizontal plastic pipe 7.5 cm in diameter, positioned ≈30 cm above cushioned bedding (Economex, Columbus, OH). The method tests the length of the time that the rat can stay on the

rotating pipe without falling. The pipe starts at zero speed and uses a constant acceleration (24).

**Monte Carlo Simulations of Dose Distributions.** The upgraded version of the code EGS4 (Electron Gamma Shower) for photon and electron transport (26) was used to calculate the dose distribution from interlaced MBs. This version included such details as the beam's linear polarization (27, 28). The work followed similar calculations made earlier (18, 19, 21).

**Imaging.** At 3 weeks, the animals were imaged by using a 9.4-T micro-MRI instrument (9.4 T/20-cm horizontal magnet interfaced to an AVANCE console; Bruker, Billerica, MA). A two-radiofrequency coil setup with a 72-mm volume resonator for spin excitation and a 30-mm surface coil for signal detection was used. T2-weighted images were acquired in the coronal plane at 1-mm slice thickness. The parameters were rare factor 8, repetition time (TR)/echo time (TE) = 2,000/40 ms, 8 averages at an in-plane resolution of 156 × 156 $\mu$m. At 6 months after the irradiation, the animals were imaged by using a Varian 4-T MRI and a custom-made micro head coil (birdcage, 5.5 cm inner diameter). Images were acquired by using gradient echo multislice imaging (T2*-weighted) at 1-mm slice thickness with no interslice gaps. The parameters were TR/TE = 550/14 ms; flip angle, 20°; and imaging matrix, 256 × 204 pixels over the field of view of 5 cm × 5 cm.

We thank M. I. Argyropoyloy, J. Dhawan, J. Escalera, B. Foerster, T. George, J. Gilbert, J. F. Hainfeld, L. Jansson, J. Kalef Ezra, S. Hussain, M. Kershaw, Y. Ma, G. M. Morris, P. Mortazavi, G. Pappas, S. Rafiq, M. Testa, M. Yu, S. Wong, M. Worth, N. Zhong, and T. Zimmerman for valuable assistance with the experiments and A. D. Woodhead for her comments on the manuscript. This work was supported by National Institutes of Health Grant R21 NS43231 and the U.S. Department of Energy (DOE). This work was carried out, in part, at the National Synchrotron Light Source, also supported by DOE Contract DE-AC02-98CH10886. Brookhaven National Laboratory is operated by the Brookhaven Science Associates under a DOE contract.

1. Slatkin, D. N., Spanne, P., Dilmanian, F. A., Gebbers, J.-O. & Laissue, J. A. (1995) *Proc. Natl. Acad. Sci. USA* **92,** 8783–8787.
2. Laissue, J. A., Geiser, G., Spanne, P. O., Dilmanian, F. A., Gebbers, J.-O., Geiser, M., Wu, X. Y., Makar, M. S., Micca, P. L., Nawrocky, M. M., *et al.* (1998) *Int. J. Cancer* **78,** 654–660.
3. Laissue, J. A., Lyubimova, N., Wagner, H. P., Archer, D. W., Slatkin, D. N., Di Michiel, M., Nemoz, C., Renier, M., Brauer, E., Spanne, P. O., *et al.* (1999) in *Medical Applications of Penetrating Radiation*, SPIE Conference Proceeding, eds. Barber, H. B. & Roehrig, H. (SPIE, Bellingham, WA), Vol. 3770, pp. 38–45.
4. Laissue, J. A., Blattmann, H., Di Michiel, M., Slatkin, D. N., Lyubimova, N., Guzman, R., Zimmermann, W., Birrer, S., Bley, T., Kircher, P., *et al.* (2001) in *Penetrating Radiation Systems and Applications III*, SPIE Conference Proceeding, eds. Barber, H. B., Roehrig, H., Doty, F. P., Schirato, R. C. & Morton, E. J. (SPIE, Bellingham, WA), Vol. 4508, pp. 65–73.
5. Dilmanian, F. A., Morris, G. M., Le Duc, G., Huang, X., Ren, B., Bacarian, T., Kalef-Ezra, J., Orion, I., Sandhu, T., Sathé, P., *et al.* (2001) *Cell. Mol. Biol.* **47,** 485–494.
6. Blattmann, H., Burkard, W., Michiel, M., Brauer, E., Stepanek, J., Bravin, A., Gebbers, J. O. & Laissue, J. A. (2002) in *Paul Scherrer Institute (PSI) Scientific Report 2001: Life Sciences*, eds. Jaussi, R. & Gschwend, B. (Paul Scherrer Inst., Villigen, Switzerland), Vol. II, p. 73.
7. Dilmanian, F. A., Button, T. M., Le Duc, G., Zhong, N., Peña, L. A., Smith, J. A. L., Martinez, S. R., Bacarian, T., Tammam, J., Ren, B., *et al.* (2002) *Neuro-Oncology* **4,** 26–38.
8. Dilmanian, F. A., Morris, G. M., Zhong, N., Bacarian, T., Hainfeld, J. F., Kalef-Ezra, J., Brewington, L., Tammam, J. & Rosen, E. M. (2003) *Radiat. Res.* **159,** 632–641.
9. Zhong, N., Morris, G. M., Bacarian, T., Rosen, E. M. & Dilmanian, F. A. (2003) *Radiat. Res.* **160,** 133–142.
10. Blattmann, H., Gebbers, J.-O., Bräuer-Krisch, E., Bravin, A., Le Duc, G., Burkard, W., Di Michiel, M., Djonov, V., Slatkin, D. N., Stepanek, J. & Laissue, J. A. (2005) *Nucl. Instrum. Methods Phys. Res. A* **548,** 17–22.
11. Dilmanian, F. A., Qu, Y., Liu, S., Cool, C. D., Gilbert, J., Hainfeld, J. F., Kruse, C. A., Laterra, J., Lenihan, D. & McDonald, J. W. (2005) *Nucl. Instrum. Methods Phys. Res. A* **548,** 30–37.
12. Bräuer-Krisch, E., Requardt, H., Régnard, P., Corde, S., Siegbahn, E. A., LeDuc, G., Blattmann, H., Laissue, J. & Bravin, A. (2005) *Nucl. Instrum. Methods Phys. Res. A* **548,** 69–71.
13. Bräuer-Krisch, E., Requardt, H., Régnard, P., Corde, S., Siegbahn, E., LeDuc, G., Brochard, T., Blattmann, H., Laissue, J. A. & Bravin, A. (2005) *Phys. Med. Biol.* **50,** 3103–3111.
14. Miura, M., Blattmann, H., Brauer-Krisch, E., Bravin, A., Hanson, A. L., Nawrocky, M. M., Micca. P. L., Slatkin, D. N. & Laissue, J. A. (2006) *Br. J. Radiol.* **79,** 71–75.
15. Smilowitz, H. M., Blattmann, H., Brauer-Krisch, E., Bravin, A., Michiel M. D., Gebbers, J. O., Hanson A. L., Lyubimova, N., Slatkin, D. N., Stepanek, J. & Laissue, J. A. (April 6, 2006) *J. Neurooncol.*, 10.1007/s11060-005-9094-9.
16. Serduc, R., Verant, P., Vial, J. C., Farion, R., Rocas, L., Remy, C., Fadlallah, T., Brauer, E., Bravin, A., Laissue, J., *et al.* (2006) *Int. J. Radiat. Oncol. Biol. Phys.* **64,** 1519–1527.
17. Denekamp, J., Dasu, A. & Waites, A. (1998) *Adv. Enzyme Regul.* **38,** 281–299.
18. Slatkin, D. N., Spanne, P., Dilmanian, F. A. & Sandborg, M. (1992) *Med. Phys.* **19,** 1395–1400.
19. Orion, I., Rozenfeld, A., Dilmanian, F. A., Telang, F., Ren, B. & Namito, Y. (2000) *Phys. Med. Biol.* ***45,*** 2497–2508.
20. Stepanek, J., Blattmann, H., Laissue, J. A., Lyubimova, N., Di Michiel, M. & Slatkin, D. N. (2000) *Med. Phys.* **27,** 1664–1675.
21. De Felici, M., Felici, R., Sanchez del Rio, M., Ferrero, C., Bacarian, T. & Dilmanian, F. A. (2005) *Med. Phys.* **32,** 2455–2463.
22. Poncelet, B. P., Wedeen, V. J., Weisskoff, R. M. & Cohen, M. S. (1992) *Radiology* **185,** 645–651.
23. O'Connor, C., Heath, D. L., Cernak, I., Nimmo, A. J. & Vink, R. (2003) *J. Neurotrauma* **20,** 985–993.
24. Buitrago, M. M., Schulz, J. B., Dichgans, J. & Luft, A. R. (2004) *Neurobiol. Learn. Mem.* **81,** 211–216.
25. Morris, G. M., Coderre, J. A., Hopewell, J. W., Rezvani, M., Micca, P. L. & Fisher, C. D. (1997) *Int. J. Radiat. Biol.* **71,** 185–192.
26. Nelson, W. R., Hirayama, H. & Rogers, D. W. O. (1985) *The EGS4 Code System* (Stanford Linear Accelerator Center, Menlo Park, CA), Report SLAC-265.
27. Namito, Y., Ban, S. & Hirayama, H. (1993) *Nucl. Instrum. Methods Phys. Res.* **332,** 277–283.
28. Namito, Y., Ban, S. & Hirayama, H. (1995) *Phys. Rev.* **51,** 3036–3043.
29. Ang, K. K., Jiang, G. L., Guttenberger, R., Thames, H. D., Stephens, L. C., Smith, C. D. & Feng, Y. (1992) *Radiother. Oncol.* **25,** 287–294.
30. Wong, C. S., Poon, J. K. & Hill, R. P. (1993) *Radiother. Oncol.* **26,** 132–138.
31. Curtis, H. J. (1967) *Radiat. Res.* **7,** Suppl., 250–257.
32. Withers, H. R., Taylor, J. M. & Maciejewski, B. (1988) *Int. J. Radiat. Oncol. Biol. Phys.* **14,** 751–759.
33. Calvo, W., Hopewell, J. W., Reinhold, H. S., van den Berg, A. P. & Yeung, T. K. (1987) *Br. J. Radiol.* **60,** 1109–1117.
34. Calvo, W., Hopewell, J. W., Reinhold, H. S. & Yeung, T. K. (1988) *Br. J. Radiol.* **61,** 1043–1052.
35. Mack, A., Wolff, R., Weltz, D., Mack, G., Jess, A., Heck, B., Czempiel, H., Kreiner, H. J., Wowra, B., Bottcher, H. & Seiffert, V. (2002) *J. Neurosurg.* **97,** Suppl., 551–555.
36. Chaves, A., Lopes, M. C., Alves, C. C., Oliveira, C., Peralta, L., Rodrigues, P. & Trindade, A. (2003) *Med. Phys.* **30,** 2904–2911.
37. Solberg, T. D., Goetsch, S. J., Selch, M. T., Melega, W., Lacan, G. & DeSalles, A. A. (2004) *J. Neurosurg.* **101,** Suppl. 3, 373–380.
38. Moskvin, V., Timmerman, R., DesRosiers, C., Randall, M., DesRosiers, P., Dittmer, P. & Papiez, L. (2004) *Phys. Med. Biol.* **49,** 4879–4895.
39. Al-Dweri, F. M. & Lallena, A. M. (2004) *Phys. Med. Biol.* **49,** 3441–3453.
40. Laster, B. H., Thomlinson, W. C. & Fairchild, R. G. (1993) *Radiat. Res.* **133,** 219–224.
41. Biston, M. C., Joubert, A., Adam, J. F., Elleaume, H., Bohic, S., Charvet, A. M., Esteve, F., Foray, N. & Balosso, J. (2004) *Cancer Res.* **64,** 2317–2323.
42. Norman, A., Ingram, M., Skillen, R. G., Freshwater, D. B., Iwamoto, K. S. & Solberg, T. (1997) *Radiat. Oncol. Invest.* **5,** 8–14.
43. Adam, J. F., Elleaume, H., Joubert, A., Biston, M. C., Charvet, A. M., Balosso, J., Le Bas, J. F. & Esteve, F. (2003) *Int. J. Radiat. Oncol. Biol. Phys.* **57,** 1413–1426.
44. Hainfeld, J. F., Slatkin, D. N. & Smilowitz, H. M. (2004) *Phys. Med. Biol.* **49,** N309–N315.
45. Hainfeld, J. F., Slatkin, D. N., Focella, T. M. & Smilowitz, H. M. (2006) *Br. J. Radiol.* **79,** 248–253.
46. Remler, M. P., Marcussen, W. H. & Sigvardt, K. (1989) *Life Sci.* **45,** 151–156.